Journal of Magnetism and Magnetic Materials 471 (2019) 274–277

Contents lists available at ScienceDirect

Journal of Magnetism and Magnetic Materials

journal homepage: www.elsevier.com/locate/jmmm

Research articles

Magnetic anisotropy of single-crystal ferromagnetic Ce_3RuSn_6

Kazuhei Wakiya[a,*], Takeru Tomaki[a], Minami Kimura[a], Masatomo Uehara[a], Jun Gouchi[b], Yoshiya Uwatoko[b], Izuru Umehara[a]

[a] Department of Physics, Yokohama National University, Yokohama 240-8501, Japan
[b] Institute for Solid State Physics, The University of Tokyo, Kashiwa 277-8581, Japan

ARTICLE INFO

Keywords:
R_3RuSn_6
Kondo effect
Non-collinear magnetic structure

ABSTRACT

Using the Czochralski pulling method, we have grown a single-crystal of orthorhombic Ce_3RuSn_6 that exhibits a ferromagnetic transition. Here we present electrical resistivity, specific heat, and magnetization measurements of this sample in the temperature range from 2 to 300 K. The electrical resistivity ρ displays a $-\ln T$ temperature dependence from 20 K to above the Curie temperature $T_C = 3$ K. At T_C, ρ decreases, and the specific heat C exhibits a sharp peak due to the magnetic transition. The magnetization measurements reveal that the magnetization M is highly anisotropic, and the magnetic structure below T_C is probably not a simple ferromagnetic structure. When the magnetic field B is applied along the b-axis or the c-axis, M shows a ferromagnetic-like rapid increase or an antiferromagnetic-like cusp anomaly, respectively, at T_C. Moreover, for $B \| c$, a metamagnetic-like anomaly appears in the magnetization curve at $B = 2.5$ T. However, for $B \| a$, M does not exhibit a distinct anomaly at T_C. The results indicate that below T_C, Ce_3RuSn_6 has a non-collinear magnetic structure and that the magnetic moments are aligned in the bc-plane.

1. Introduction

Over the last three decades, cerium-based intermetallic compounds have attracted much attention because they exhibit a wide variety of strongly correlated phenomena, e.g., the formation of heavy fermion states, non-Fermi liquid behavior, and pressure-induced superconductivity [1]. It is well-established that these phenomena occur as a result of the competition between Ruderman-Kittel-Kasuya-Yosida (RKKY) type interactions and the Kondo effect caused by the hybridization of the conduction and 4*f* electrons (*c*-*f* hybridization) [1,2].

Gribanova et al. recently reported that Ce_3RuSn_6, which has the orthorhombic Yb_3CoSn_6-type structure (space group Cmcm, #63) [3], undergoes a ferromagnetic transition at the Curie temperature $T_C = 3$ K [4]. The crystal structure of Ce_3RuSn_6, as depicted by the VESTA program [5], is shown in Fig. 1(a). The Ce atoms occupy 4*c* and 8*f* sites and form AlB_2-type slabs with the Sn atoms, although the triangles composed of Ce atoms are slightly distorted from regular triangles [Fig. 1(b)] [4]. In this compound, a steep, ferromagnetic-like rise of the magnetization and a specific–heat peak have been observed at $T_C = 3$ K. The magnetic entropy reaches 72% of $3R\ln 2$ [J/K mol] at T_C, implying that the magnetic transition is caused by the magnetic moments of the Ce atoms at both the 4*c* and 8*f* sites. Furthermore, Ce_3RuSn_6 exhibits a Kondo-type behavior in its electrical resistivity and specific heat. The electrical resistivity shows a $-\ln T$ dependence below 20 K, and the Sommerfeld coefficient γ is 330 [mJ/K^2 Ce mol], as determined from the specific heat. In addition, Upadhyay et al. [6] reported that isostructural R_3RuSn_6 (R = Gd and Tb) exhibits at least two magnetic transitions, and they suggested strong *c*-*f* hybridization in Ce_3RuSn_6 from the breakdown of de Gennes scaling. These observations suggest that Ce_3RuSn_6 is a rare example that shows a ferromagnetic transition with strong influence from the Kondo effect. However, it is still unclear whether the magnetic structure is simply ferromagnetic, because the earlier research was performed on polycrystalline samples.

This study aims to gain further insight into the magnetic properties of Ce_3RuSn_6 by emphasizing particularly the magnetic structure below T_C. We have grown single-crystal Ce_3RuSn_6 using the Czochralski pulling method and have measured its electrical resistivity, specific heat, and magnetization. The measurements show that the magnetic structure of Ce_3RuSn_6 does not resemble a simple ferromagnet but rather exhibits a complex magnetic structure below T_C.

2. Experimental procedure

The single-crystal of Ce_3RuSn_6 was prepared via the Czochralski pulling method using a tetra arc crystal furnace. Pure elements of Ce (99.9%), Ru(99.99%), and Sn(99.999%) in stoichiometric amounts

* Corresponding author.
E-mail address: wakiya-kazuhei-tz@ynu.ac.jp (K. Wakiya).

https://doi.org/10.1016/j.jmmm.2018.09.018
Received 30 May 2018; Received in revised form 27 August 2018; Accepted 5 September 2018
Available online 06 September 2018
0304-8853/

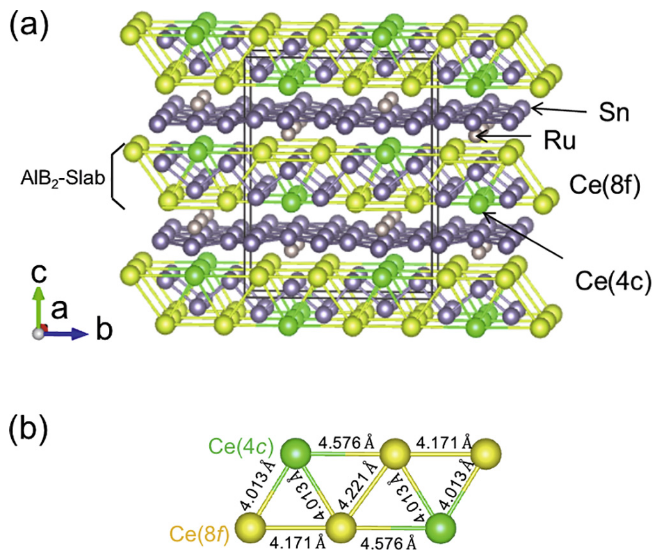

Fig. 1. (a) Crystal structure of Ce_3RuSn_6 as depicted by VESTA program [5]. (b) The distances between the centers: Ce(4*c*)-Ce(8*f*) and Ce(8*f*)-Ce(8*f*) [4].

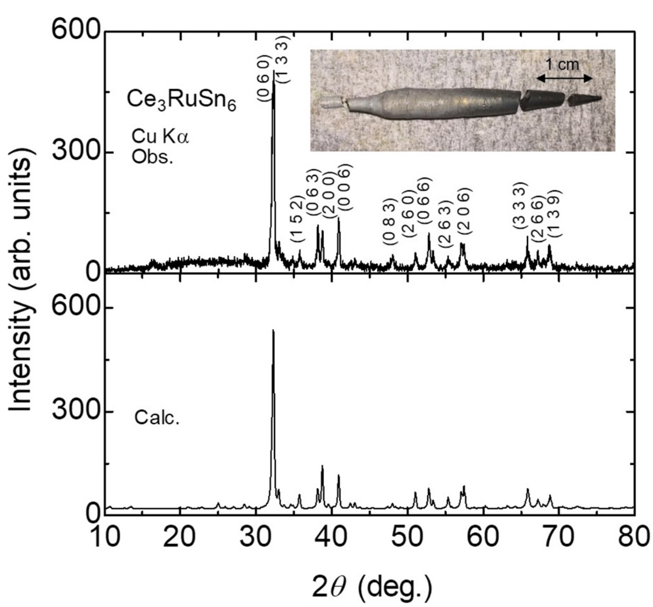

Fig. 2. Powder X-ray diffraction pattern of Ce_3RuSn_6. The inset shows a photograph of the grown sample.

(~20 g) were used as the starting materials. Before growing the single crystal, Ce_3RuSn_6 polycrystals were made preliminary using a mono arc furnace. A photograph of the grown sample is shown in the inset of Fig. 2. To characterize the sample, we crushed part of it and performed powder X-ray diffraction measurements using a Rigaku mini-flex II X-ray diffractometer. As shown in Fig. 2, the peaks in the powder X-ray diffraction pattern can be indexed to the Yb_3CoSn_6-type structure. The lattice parameters were determined to be $a = 4.676$ Å, $b = 16.853$ Å, and $c = 13.316$ Å. These values agree with the values reported for a polycrystalline sample [4]. The directions of the crystal axes were determined from the back-scattered Laue pattern. The Laue diffraction measurements revealed that this sample consists of at least two grains. We cut a single-grain sample with a size of $1\times0.5\times2\,mm^3$ from the grown sample and used it for measurements of the electrical resistivity, magnetization, and specific heat.

Electrical resistivity was measured by a conventional DC four-probe method in a liquid-helium free refrigerator (FR-TL-R-10; Fujihira Co., Ltd.) over the temperature range 2–280 K. The current flow was chosen

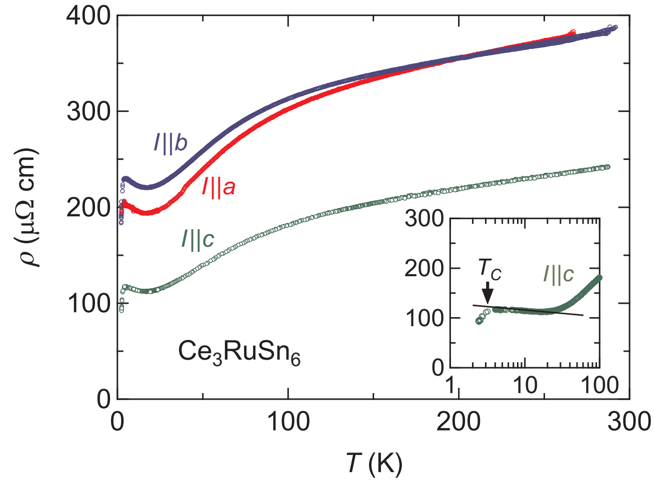

Fig. 3. Temperature dependence of the electrical resistivity $\rho(T)$ for Ce_3RuSn_6 with the current along the a-, b-, and c-axes. The inset shows the logρ-log$T$ dependence for current flowing along the c-axis.

along one of the three principal crystallographic axes. Magnetization as a function of magnetic field (up to 5 T) and temperature (from 2 to 300 K) was measured using a superconducting quantum interference device magnetometers (Quantum Design, MPMS and Cryogenic Limited, S700X-R). For these measurements, the sample was fixed on a homemade holder using Apiezon grease to avoid rotation of the sample caused by the magnetic torque. Specific heat was measured by the thermal relaxation method (Quantum Design, PPMS) at temperatures in the range 2–300 K.

3. Results and discussion

Fig. 3 shows the temperature dependence of the electrical resistivity $\rho(T)$ for Ce_3RuSn_6, with the current flow directed along each of the principal crystallographic orientations separately. Overall, $\rho(T)$ does not depend on the current direction, except for the values of the residual resistivity $\rho(2\ \mathrm{K})$. On cooling, ρ decreases monotonically down to 20 K and then displays an upturn that is a characteristic feature of Kondo scattering. As shown in the inset of Fig. 3, ρ falls at around $T_C = 3$ K due to the magnetic transition. This behavior agrees well with that in the polycrystalline samples, as reported earlier [4,7]. However, the residual resistivity $\rho(2\mathrm{K})$ is approximately 5–10 times smaller than that of the polycrystalline sample [4], indicating the better crystalline quality of the present sample.

The temperature dependence of the specific heat $C(T)$ for Ce_3RuSn_6 is shown in Fig. 4. At room temperature, $C(T)$ approaches the Dulong-Petit limit for $3nR = 249.43$ [J/K mol], where R is the gas constant and n (= 10) is the number of atoms per formula unit. This fact also supports our conclusion that the main phase of this sample is Ce_3RuSn_6. At $T_C = 3$ K, $C(T)$ exhibits a peak corresponding to the magnetic transition. As shown in the inset of Fig. 4, the peak at T_C in a plot of C/T vs T for the single crystal is well-defined, providing further evidence of the higher crystalline quality of the present sample. At the same time, the tail above T_C is observed regardless of the sample crystallinity, thus indicating that this feature is intrinsic and may result from short-range correlations between the magnetic moments.

Fig. 5 shows the temperature dependence of the magnetic susceptibility χ (left-hand scale) and the inverse magnetic susceptibility χ^{-1} (right-hand scale) measured in a magnetic field $B = 1$ T. Above 200 K, χ follows the Curie–Weiss law, $B/M = (T-\theta_p)/C$, where C is the Curie constant and θ_p is the Weiss temperature. From Curie–Weiss fits, we determined the effective magnetic moment μ_{eff} and θ_p to be $\mu_{eff} = 2.63\ \mu_B$/Ce and $\theta_a = -71$ K for $B||a$; $\mu_{eff} = 2.49\ \mu_B$/Ce and $\theta_b = -3.1$ K for $B||b$; and $\mu_{eff} = 2.57\ \mu_B$/Ce and $\theta_c = -1.5$ K for $B||c$. The values of μ_{eff}